JOURNAL OF THERMOPHYSICS AND HEAT TRANSFER
Vol. 10, No. 3, July–August 1996

Steady-State Analysis of the Conjugate Heat Transfer Between Forced Counterflowing Streams

C. Treviño,* A. Espinoza,† and F. Méndez‡
Univerídad Nacional Autonoma De Mexico, 04510 D. F., Mexico

In this article we analyze the steady-state conjugate heat transfer process between two counterflowing forced streams separated by a wall with finite thermal conductivity. The influence of the longitudinal heat conduction through the wall is very important on the overall heat transfer rates and has been analytically deduced. The most important parameters are denoted by α, β, and ε. The parameter α corresponds to the ratio of the solid heat conduction in the longitudinal direction to the convected heat towards the hotter fluid, β is the relationship between the thermal boundary-layer thickness of both fluids, and ε is the aspect ratio of the plate. In the asymptotic limit $\alpha \to \infty$ and using the Lighthill approximation, it can be shown that the balance equations reduce to a single integro-differential equation with only the parameters α and β. This limit is analyzed using regular perturbation techniques. On the other hand, for $\alpha \to 0$, the governing equations can also be solved using asymptotic methods. The distribution of the temperature of the plate as well as the overall heat transfer rates have been obtained in closed form and compared with the numerical solution for different values of the parametric set. In general, close to the analyzed limits, a good agreement is achieved.

I. Introduction

THE study of conjugate heat transfer between forced convection flows and conduction in walls is important because of the existence of coupled effects in practical heat transfer processes. In particular, the design and performance of counterflow multilayered heat exchangers offer an excellent opportunity to analyze these phenomena. Research on fin's efficiency, double pipe, and parallel plate exchangers are progressing because of the simple geometry and the well-known flow conditions in these heat exchanger types. In connection with the conjugate heat transfer process over surfaces, the effects of wall heat conduction and convective heat transfer have been analyzed in several works. Luikov[1] and Payvar[2] analyzed the conjugate problem where the lower surface of a horizontal flat plate of finite thickness is maintained at a uniform temperature, while heat is convected to a laminar boundary layer at the upper surface of the plate. They neglected the longitudinal heat conduction in the solid. Luikov[1] developed two approximate solutions, one based on a differential analysis with low Prandtl number and the second based on an integral analysis with assumed polynomial forms for the velocity and temperature profiles. He concluded that for Brun numbers larger than 0.1, the thermal resistance can be neglected. Payvar[2] used the Lighthill approximation[3] for large Prandtl numbers to obtain an integral equation that has been solved numerically. He obtained asymptotic solutions for large and small Brun numbers.

The process of heating (or cooling) of a flat plate in a convective flow was studied by Sohal and Howell[4] and Karvinen.[5] Both works used the Lighthill approximation to obtain an integro-differential equation. In particular, Sohal and Howell[4] used a numerical scheme to solve the governing equation, whereas Karvinen[5] used an iterative method to solve the integro-differential equation by including the steady-state and transient solutions. He obtained good qualitative agreement with experimental results. On the other hand, perturbation techniques were employed to solve analytically the integro-differential equation resulting from the externally heated flat plate in convective flow.[6] This equation has only one parameter, α, which corresponds to the ratio of the solid heat conduction to the convected heat towards the hotter fluid, and is inversely proportional to the Brun number. For large values of α (very good conducting plate), a regular perturbation approach is applied using $1/\alpha$ as the small parameter of expansion. Otherwise, for very small values of this parameter, a singular perturbation technique has been employed (matched asymptotic expansions) to study the plate temperature evolution. The leading term of the expansion ($\alpha = 0$) has a self-similar solution and the resulting integral equation has been numerically solved. For small values of α, two boundary layers develop at both edges of the plate. These boundary layers, however, have only local effects and the leading-order solution gives accurate results for small values of α, even for this singular problem. They also included the cooling process for $\alpha = 0$. However, for the case of large values of α, the cooling process cannot be analyzed using the same regular perturbation techniques used by Treviño and Liñán,[6] because this series breaks down in the first-order terms. Vallejo and Treviño[7] analyzed the cooling process of a plate in a convective flow using multiple scales asymptotic techniques. The main conclusion of these works is that the longitudinal heat conduction must be retained to estimate correctly the global heat transfer rates.

For a heat exchanger problem between two fully developed laminar streams, Stein[8] presented an analysis for coflowing, double-pipe heat exchangers. He obtained the heat transfer coefficient in the range where a thermal boundary layer was established. A few years later, Nunge and Gill[9] treated the same problem for both coflowing and counterflowing cases, deriving a new orthogonal relation, and giving the local Nusselt number distributions. Nunge et al.[10] made an analysis of parallel plate exchangers where the longitudinal conduction was taken into account in the flowing fluids. They found that the local Nusselt number of each stream was different from the usual, single-stream problem and that each number was affected by the existence of the other stream. Their more relevant conclusion showed that there was not a big influence of the longitudinal heat conduction in the fluid for Peclet numbers of 100 or more.

Received Aug. 22, 1995; revision received Jan. 25, 1996; accepted for publication Jan. 26, 1996.

*Professor, Facultad de Ciencias.

†Professor, Facultad de Ciencias; on sabbatical leave from the Escuela de Física, UAZ, Zacatecas, Mexico.

‡Professor, Facultad de Ingeniería.

Mori et al.[11] analyzed theoretically multilayered parallel plate heat exchangers under laminar flow conditions. Their conclusion is that in the examination of mixed-mean temperature distributions, the longitudinal wall conduction significantly reduces exchanger effectiveness in the low-Grätz number region. Note that the last four works just mentioned have appeared as extensions of the classical Grätz problem.

The objective of the present work is to obtain analytically the overall heat transfer rates and the temperature profiles in the wall, which separates two counterflowing forced flow streams at different temperatures. The set of governing equations are elliptic because of the existing counterflow pattern, even if the axial wall heat conduction effects were not taken into account. Using the Lighthill asymptotic approximation for large Prandtl numbers of both streams, we show that the energy equation for the flat plate depends fundamentally on three parameters: α and β representing the ratio of the thermal resistances on both fluids and the aspect ratio of the plate ε. The nondimensional parameters are to be defined in the following section. We use asymptotic techniques exploring analytically the limiting cases of large and small values of α for values of β of order unity, and small values of ε and compare with the numerical solution obtained using a code described elsewhere (Medina et al.[12]). To the knowledge of the authors, no experimental results on the physical problem analyzed here have been published. The analysis made in this work can be easily extended to study the heat transfer process between counterflowing fluids in concentric tubes, assuming that the thermal-layer thicknesses are much smaller than the diameter of the inner tube.

II. Formulation

The physical model under study is shown in Fig. 1. A thin flat plate of length L and thickness h is placed between two counterflowing streams with freestream velocities and temperatures $(U_{I\infty}, T_{I\infty})$ and $(U_{II\infty}, T_{II\infty})$, for the upper and lower streams, respectively. The upper left corner of the plate coincides with the origin of a Cartesian coordinate system whose y axis points upward in the direction normal to the plate and its x axis points to the right in the plate's longitudinal direction. For large Reynolds numbers of both flows ($Re_i = U_{i\infty}L/\nu_i$, $i = I, II$), two viscous-nonisothermal boundary layers develop, with characteristic thicknesses related to the length of the plate of the order of the inverse of the square root of the corresponding Reynolds numbers, for the upper and lower flows, respectively. It will be assumed, without any loss of generality, that the temperature of the upper fluid is higher than that of the lower fluid, $T_{I\infty} > T_{II\infty}$.

For fluids with Prandtl numbers of order unity or larger, $Pr_i = \rho_i \nu_i c_i/\lambda_i$, the characteristic thicknesses of both thermal boundary layers are of the order

$$\delta_i \sim \frac{L}{Pr_i^{1/3} Re_i^{1/2}} \quad \text{for} \quad i = I, II$$

Here, ρ_i, ν_i, c_i, and λ_i denote the density, kinematic viscosity, specific heat, and thermal conductivity of the fluid i, respectively.

The orders of magnitude of the heat fluxes across the boundary layers in the fluids are

$$q_i \sim \frac{\lambda_i \Delta T_i Re_i^{1/2} Pr_i^{1/3}}{L} \quad \text{for} \quad i = I, II \tag{1}$$

where ΔT_i ($i = I, II$) are the transversal characteristic temperature changes in the fluids, $\Delta T_i = |T_{i\infty} - T_{wi}|$. Here, T_{wi} represents the characteristic temperature of the plate surface facing fluid i. If we assume both edges of the plate to be adiabatic, then the heat flux from fluid I to the wall is of the same order

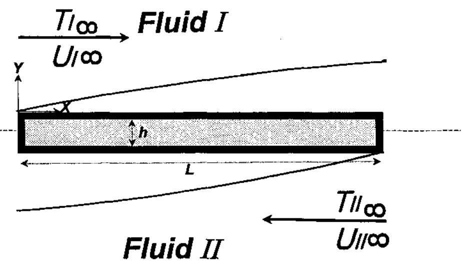

Fig. 1 Schematic diagram of the studied physical model.

of magnitude as the heat flux from the wall to fluid II and also transversely in the wall, i.e.,

$$q_I \sim q_{II} \sim q_w \tag{2}$$

or

$$\frac{\lambda_I \Delta T_I Re_I^{1/2} Pr_I^{1/3}}{L} \sim \frac{\lambda_{II} \Delta T_{II} Re_{II}^{1/2} Pr_{II}^{1/3}}{L} \sim \frac{\lambda_w \Delta T_w}{h} \tag{3}$$

In these relationships, ρ_w, c_w, and λ_w represent the density, specific heat, and thermal conductivity of the wall material, respectively. ΔT_w is the characteristic transversal temperature drop at the wall, $\Delta T_w = |T_{wI} - T_{wII}|$. From Eq. (3) we obtain the ratio of the characteristic temperature drop in the boundary layers of both fluids to the characteristic temperature drop at the wall as

$$\frac{\Delta T_I}{\Delta T_w} \sim \frac{\alpha}{\varepsilon^2} \quad \text{and} \quad \frac{\Delta T_{II}}{\Delta T_w} \sim \frac{\alpha}{\varepsilon^2 \beta} \tag{4}$$

where

$$\alpha = \frac{1}{0.332} \frac{\lambda_w}{\lambda_I} \frac{h}{L} \frac{1}{Re_I^{1/2} Pr_I^{1/3}}, \quad \beta = \frac{\lambda_{II} Re_{II}^{1/2} Pr_{II}^{1/3}}{\lambda_I Re_I^{1/2} Pr_I^{1/3}} \quad \text{and} \quad \varepsilon = \frac{h}{L} \tag{5}$$

which represent the most relevant nondimensional parameters for this problem. Here, α is a nondimensional parameter that relates the solid heat conduction to the convective heat towards the upper fluid, β represents the relationship between the thermal boundary-layer thickness of the lower fluid to that of the upper fluid, and ε represents the aspect ratio of the plate. The value of β will be assumed to be of order unity throughout this article, except in the cases where it is explicitly mentioned. Using the fact that

$$\Delta T_I + \Delta T_{II} + \Delta T_w \sim \Delta T = T_{I\infty} - T_{II\infty}$$

from Eq. (4) we obtain a single relationship for the order of magnitude of $\Delta T_w/\Delta T$ as

$$\frac{\Delta T_w}{\Delta T} \sim \left[1 + \frac{\alpha}{\varepsilon^2}\left(1 + \frac{1}{\beta}\right)\right]^{-1} \tag{6}$$

To evaluate the effect of longitudinal heat conduction on the overall heat transfer process, we must compare the heat transfer by conduction along the solid, which is of the order $h(\lambda_w \Delta T_{Lw}/L)$ (with ΔT_{Lw} denoting the characteristic temperature change along the solid), with the heat transfer from the fluids to the solid, of the order $L(\lambda_w \Delta T_w/h)$. The ratio of the two is $R \sim \varepsilon^2 \Delta T_{Lw}/\Delta T_w$ or, using Eq. (6),

$$R \sim \frac{\alpha(1 + \beta)}{\beta} \frac{\Delta T_{Lw}}{\Delta T} \quad \text{for} \quad \frac{\alpha}{\varepsilon^2} \gg 1 \tag{7}$$

which is independent of ε. The longitudinal heat conduction effects are important for values of R of order unity. In this case Eq. (7) implies

$$\frac{\Delta T_{Lw}}{\Delta T} \sim \frac{\beta}{\alpha(1+\beta)} \tag{8}$$

Thus, the ratio $\Delta T_{Lw}/\Delta T$ should be of the order $1/\alpha$ for large values of α compared with unity. As the value of α decreases reaching values of order unity, $\Delta T_{Lw}/\Delta T$ becomes also of order unity. Because the maximum value of this ratio is unity, then $R \sim \alpha(1+\beta)/\beta$, for values of $\alpha < 1$. Thus, the longitudinal heat conduction ceases to be important for values of $\alpha \ll \beta/(1+\beta)$.

For large values of α/ε^2 (thermally thin wall approximation), the wall temperature variations in the transversal direction are very small compared with the overall temperature difference ΔT, as shown by Eq. (6). In this limit, the wall temperature can be assumed to be a function only of the longitudinal direction. The nondimensional heat flux or overall Nusselt number in this regime asymptotically reaches a constant that can be obtained by the following definition:

$$\overline{Nu} = \frac{1}{0.332Re_I^{1/2}Pr_I^{1/3}} \frac{\overline{q_w}L}{\lambda_{I\infty}(T_{I\infty} - T_{II\infty})} \sim \frac{\beta}{1+\beta} \tag{9}$$

where

$$\overline{q_w} = \frac{1}{L}\int_0^L q_w(x)\,\mathrm{d}x$$

On the other hand, for values of α/ε^2 of order unity (thermally thick wall approximation), the wall temperature change in the transversal direction is of the same order as ΔT and the longitudinal heat conduction term in the wall can be neglected, because in general as assumed in this work, ε is a small number. The limiting value of the nondimensional heat flux or overall Nusselt number in this regime gives

$$\overline{Nu} \sim (\alpha/\varepsilon^2), \quad \text{for} \quad (\alpha/\varepsilon^2) \to 0$$

Introducing the following normalized variables:

$$\theta = \frac{T - T_{II\infty}}{T_{I\infty} - T_{II\infty}}, \qquad \chi = \frac{x}{L}, \qquad z = \frac{y}{h} \tag{10}$$

the nondimensional energy equation for the plate is given by the well-known Laplace equation:

$$\frac{\partial^2\theta}{\partial\chi^2} + \frac{1}{\varepsilon^2}\frac{\partial^2\theta}{\partial z^2} = 0 \tag{11}$$

We assume for simplicity that both edges (leading and trailing edges) are adiabatic, which correspond to the boundary conditions given by

$$\frac{\partial\theta}{\partial\chi} = 0 \quad \text{at} \quad \chi = 0 \quad \text{and} \quad \chi = 1 \tag{12}$$

The boundary conditions at the upper and lower solid–fluid interfaces are obtained from continuity of the temperature and the heat flux. Using the asymptotic Lighthill approximation[3] valid for large Prandtl numbers compared with unity, these nonlinear boundary conditions are given by

$$\left.\frac{\partial\theta}{\partial z}\right|_{z=0} = \frac{\varepsilon^2}{\alpha}\frac{1}{\sqrt{\chi}}\left(1 - \theta_{lu} - \int_0^\chi K_u \frac{\mathrm{d}\theta_u'}{\mathrm{d}\chi'}\,\mathrm{d}\chi'\right) \tag{13}$$

$$\left.\frac{\partial\theta}{\partial z}\right|_{z=-1} = \frac{\varepsilon^2}{\alpha}\frac{\beta}{\sqrt{1-\chi}}\left(\theta_{ld} + \int_1^\chi K_d \frac{\mathrm{d}\theta_d'}{\mathrm{d}\chi'}\,\mathrm{d}\chi'\right) \tag{14}$$

The Lighthill approximation gives accurate results also for values of the Prandtl number of order unity. The Kernels of the integrals in the previous equations are given by

$$K_u = [1 - (\chi'/\chi)^{3/4}]^{-1/3}$$
$$K_d = \{1 - [(1-\chi')/(1-\chi)]^{3/4}\}^{-1/3} \tag{15}$$

where the subindex u and d denote the upper and lower interfaces and l denotes the leading edge. For the upper fluid the leading edge corresponds to the left one, whereas for the lower fluid it is the right one.

For large values of α, that is, $\alpha \gg 1$, the heat conducted by the plate is very large in all directions, thus, no temperature gradients of importance arise in the wall. In this limit the nondimensional transversal variations of the wall temperature are very small compared with the corresponding longitudinal variations, which are of order $1/\alpha$ as predicted by the order of magnitude estimate (8). On the other hand, for $\alpha \ll 1$, the heat convected from the fluids is extremely important, and large nondimensional temperature gradients occur mainly in the transversal direction and the longitudinal heat conduction can be neglected. In this article we analyze the conjugate problem using asymptotic techniques for values of the parameter $\alpha \gg 1$ and $\alpha/\varepsilon^2 \ll 1$, $\beta \sim 1$ with $\varepsilon \ll 1$ and numerical techniques for the whole parametric space.

III. Thermally Thin Wall Regime ($\alpha/\varepsilon^2 \gg 1$)

This regime is very important and applies to most practical cases of metallic plates. Integrating the Laplace Eq. (11) in the transversal direction and applying the boundary conditions at the fluid–solid interfaces (13) and (14), we obtain the reduced nondimensional energy equation in the form

$$\alpha\frac{\mathrm{d}^2\theta}{\mathrm{d}\chi^2} = -\frac{1}{\sqrt{\chi}}\left[1 - \theta(0) - \int_0^\chi K_u\frac{\mathrm{d}\theta'}{\mathrm{d}\chi'}\,\mathrm{d}\chi'\right] + \frac{\beta}{\sqrt{1-\chi}}\left[\theta(1) + \int_1^\chi K_d\frac{\mathrm{d}\theta'}{\mathrm{d}\chi'}\,\mathrm{d}\chi'\right] \tag{16}$$

where we assumed that $\int_{-1}^{0}\theta(\chi,z)\,\mathrm{d}z \simeq \theta_u(\chi) \simeq \theta_d(\chi) \simeq \theta(\chi)$. This equation is to be solved with the corresponding adiabatic conditions at both edges.

For very large values of the parameter α compared with unity, the nondimensional temperature of the plate changes very little in the longitudinal direction of order α^{-1}. This limit is regular and is to be analyzed using α^{-1} as the small parameter of expansion. For very thin plates, such as $\varepsilon \ll 1/\sqrt{\alpha}$, the temperature of the plate can be expanded by the following asymptotic series:

$$\theta(\alpha,\chi) = \sum_{j=0}^{\infty}\frac{1}{\alpha^j}\theta_j(\chi) \tag{17}$$

Introducing the previous relationship into the nondimensional governing Eqs. (16) and (12), we obtain the following equations:

$$\frac{\mathrm{d}^2\theta_0}{\mathrm{d}\chi^2} = 0 \tag{18}$$

$$\frac{\mathrm{d}^2\theta_1}{\mathrm{d}\chi^2} = -\frac{1}{\sqrt{\chi}}\left[1 - \theta_0(0) - \int_0^\chi K_u\frac{\mathrm{d}\theta_0'}{\mathrm{d}\chi'}\,\mathrm{d}\chi'\right] + \frac{\beta}{\sqrt{1-\chi}}\left[\theta_0(1) + \int_1^\chi K_d\frac{\mathrm{d}\theta_0'}{\mathrm{d}\chi'}\,\mathrm{d}\chi'\right] \tag{19}$$

$$\frac{d^2\theta_{n+1}}{d\chi^2} = \frac{1}{\sqrt{\chi}}\left[\theta_n(0) + \int_0^\chi K_u \frac{d\theta_n'}{d\chi'} d\chi'\right] + \frac{\beta}{\sqrt{1-\chi}}\left[\theta_n(1) + \int_1^\chi K_d \frac{d\theta_n'}{d\chi'} d\chi'\right] \tag{20}$$

for $n \geq 1$, and

$$\frac{d\theta_n}{d\chi} = 0 \quad \text{at} \quad \chi = 0 \quad \text{and} \quad 1 \quad \text{for all } n \tag{21}$$

Solving Eqs. (18) and (21) gives a constant for θ_0, which can be found after integrating the following higher-order Eq. (19) with the corresponding adiabatic conditions at both edges. In this form, the solution for θ_0 is given by

$$\theta_0 = 1/(1+\beta) \tag{22}$$

The solution to Eq. (19) is

$$\theta_1(\chi) = [4\beta/3(1+\beta)][\tfrac{3}{2}\chi + (1-\chi)^{3/2} - \chi^{3/2} + A] \tag{23}$$

where A is to be found again after integration of the next higher Eq. (20) for $n = 1$. This gives

$$A = -[1/(1+\beta)][(1-a) + \beta(\tfrac{1}{2} + a)] \tag{24}$$

where $a = 0.2695\ldots$. Using the same procedure, $\theta_2(\chi)$ can be obtained, giving

$$\theta_2(\chi) = D + C\chi + \frac{4}{3}\theta_1(0)\chi^{3/2} + \frac{4}{3}\beta\theta_1(1)(1-\chi)^{3/2} + \frac{8\beta}{3(1+\beta)}\left\{-\frac{1}{6}B\left(2, \frac{2}{3}\right)[\chi^3 - \beta(1-\chi)^3] + 2\sum_{n=1}^{\infty}\frac{a_n}{2n+5}[\chi^{(2n+5)/2} - \beta(1-\chi)^{(2n+5)/2}]\right\} \tag{25}$$

where

$$C = \frac{4}{3}\frac{(4a-1)\beta^2}{(1+\beta)^2} \tag{26}$$

$$a_n = \frac{1}{2^{2n-2}}\frac{1}{(2n+3)}\frac{(2n-2)!}{n!(n-1)!}B\left(\frac{4n+4}{3}, \frac{2}{3}\right) \tag{27}$$

$$D = \frac{1}{1+\beta}\left\{-\frac{4}{3}\beta r[\theta_1(0) + \theta_1(1)] - \frac{2}{3}B\left(2, \frac{2}{3}\right) \times [\theta_1(0) + \beta^2\theta_1(1)] - \beta C - \frac{4}{9}(1-\beta)CB\left(\frac{4}{3}, \frac{2}{3}\right) + \frac{32}{9}\beta(1-\beta)m\right\} \tag{28}$$

with $r = 0.3707\ldots$, and $m = 0.02529\ldots$. $B(f, g)$ corresponds to the Beta function. Using the series expansion (17), the overall reduced Nusselt number given by

$$\overline{Nu} = \frac{\alpha}{\varepsilon^2}\int_0^1 \left.\frac{\partial\theta}{\partial z}\right|_{z=0} d\chi \tag{29}$$

can also be expanded in the following form:

$$\overline{Nu} = 2\left[\frac{\beta}{1+\beta} + \frac{2(4a-1)\beta^2}{3\alpha(1+\beta)^2} + \frac{G(\beta)}{\alpha^2} + \mathcal{O}(\alpha^{-3})\right] \tag{30}$$

where

$$G(\beta) = -\theta_2(0) - \frac{4}{3}\left\{\frac{1}{2}\theta_1(0)B\left(2, \frac{2}{3}\right) - 2\beta\theta_1(1)\left[\frac{1}{3}B\left(\frac{4}{3}, \frac{2}{3}\right) - \frac{1}{2}\sum_{n=1}^{\infty}a_n\right] + \frac{8\beta}{3(1+\beta)}\left\{-\frac{1}{2}B\left(2, \frac{2}{3}\right)\left[\frac{\beta+1}{7}B\left(4, \frac{2}{3}\right) + \frac{\beta}{3}B\left(\frac{4}{3}, \frac{2}{3}\right) - \frac{2\beta}{5}B\left(\frac{8}{3}, \frac{2}{3}\right)\right] + \frac{1}{2}\sum_{n=1}^{\infty}\frac{a_n}{n+3} \times B\left(\frac{4n+10}{3}, \frac{2}{3}\right) + \beta\sum_{n=1}^{\infty}\sum_{m=0}^{n+2}\frac{a_n d_{mn}}{2m+3} \times B\left(\frac{4m+4}{3}, \frac{2}{3}\right) + \beta\sum_{n=1}^{\infty}\sum_{m=n+3}^{\infty}\frac{a_n e_{mn}}{2m+3} \times B\left(\frac{4m+4}{3}, \frac{2}{3}\right)\right\} + \frac{C}{3}B\left(\frac{4}{3}, \frac{2}{3}\right)\right\}$$

$$d_{mn} = \frac{(-1)^m(2n+3)!(n-m+2)!}{2^{2m-1}m!(2n-2m+4)!(n+1)!}$$

$$e_{mn} = \frac{(-1)^n(2n+3)!(2m-2n-4)!}{2^{2m-1}m!(m-n-2)!(n+1)!}$$

IV. Thermally Thick Wall Regime ($\alpha/\varepsilon^2 \sim 1$)

For values of $\alpha/\varepsilon^2 \sim 1$, the transversal temperature variations in the plate are now very important and must be retained. In this regime $\alpha \sim \varepsilon^2 \ll 1$, and therefore, the longitudinal heat conduction in the plate is very small. Neglecting the longitudinal heat conduction in this limit is possible in the whole length of the wall, except in regions of order ε close to $\chi = 0$ and $\chi = 1$, because the adiabatic boundary conditions cannot be satisfied. However, these layers have only local effects and don't modify substantially the results for small values of ε. We avoid presenting the inner structure of these layers. The temperature profiles in the transversal direction of the plate are linear of the form

$$\theta(\chi, z) = \theta_u(\chi)(1+z) - \theta_d(\chi)z \tag{31}$$

Therefore, the energy equation for the plate represented by Eqs. (13) and (14) now take the form

$$\theta_u - \theta_d = -\frac{\varepsilon^2}{\alpha}\frac{1}{\sqrt{\chi}}\left(\int_0^\chi K_u\frac{d\theta_u'}{d\chi'}d\chi'\right) = \frac{\varepsilon^2}{\alpha}\frac{\beta}{\sqrt{1-\chi}}\left(\int_1^\chi K_d\frac{d\theta_d'}{d\chi'}d\chi'\right) \tag{32}$$

with the conditions $\theta_u(0) = 1$ and $\theta_d(1) = 0$. These equations are still elliptic even without the inclusion of the longitudinal heat conduction term in the wall.

A. Asymptotic Limit $\alpha/\varepsilon^2 \ll 1$

The limiting case $\alpha/\varepsilon^2 \to 0$ is singular because the Nusselt number goes to zero as α tends to 0. However, the local nondimensional temperature gradient defined by Eq. (13) tends to a finite value as $\alpha/\varepsilon^2 \to 0$. Thus, this problem can be analyzed using regular perturbation techniques with α/ε^2 as the small parameter of expansion. For $\alpha/\varepsilon^2 = 0$, we obtain a linear profile in z for the nondimensional temperature of the plate without any heat flux (perfect isolated wall). We assume a solution for the nondimensional plate temperature given by Eq. (31) with

$$\theta_u(\chi) = 1 + \frac{\alpha}{\varepsilon^2}a(\chi) + \frac{\alpha^2}{\varepsilon^4}c(\chi) + \mathcal{O}(\alpha^3/\varepsilon^6) \tag{33}$$

$$\theta_d(\chi) = (\alpha/\varepsilon^2)[a(\chi) - b(\chi)] + (\alpha^2/\varepsilon^4)[c(\chi) - d(\chi)] + \mathcal{O}(\alpha^3/\varepsilon^6) \tag{34}$$

These relationships have to be introduced into the nondimensional Laplace Eq. (32). Using Abel's inversion, we obtain after comparing terms with the same power of α/ε^2:

$$a(\chi) = -k\sqrt{\chi} \tag{35}$$

$$b(\chi) = -k[\sqrt{\chi} + (1/\beta)\sqrt{1-\chi}] \tag{36}$$

$$c(\chi) = \frac{3k}{2\beta}\left[\frac{1}{B(\frac{2}{3}, \frac{2}{3})}\chi^{1/2} + \frac{\beta}{2B(\frac{4}{3}, \frac{2}{3})}\chi - \sum_{n=1}^{\infty} c_n\chi^{(2n+1)/2}\right] \tag{37}$$

$$\begin{aligned} d(\chi) = \frac{3k}{2\beta}\Bigg\{&\frac{1}{B(\frac{2}{3}, \frac{2}{3})}[\chi^{1/2} + (1-\chi)^{1/2}] \\ &+ \frac{1}{2B(\frac{4}{3}, \frac{2}{3})}\left[\beta\chi + \frac{1}{\beta}(1-\chi)\right] \\ &- \sum_{n=1}^{\infty} c_n[\chi^{(2n+1)/2} + (1-\chi)^{(2n+1)/2}]\Bigg\} \end{aligned} \tag{38}$$

where

$$c_n = \frac{1}{2^{2n-1}}\frac{1}{(2n+1)}\frac{(2n-2)!}{n!(n-1)!}\left[B\left(\frac{4n+2}{3}, \frac{2}{3}\right)\right]^{-1} \tag{39}$$

$$k = (\sqrt{3}/2\pi)B(\tfrac{4}{3}, \tfrac{1}{3}) \simeq 0.730266\ldots$$

The overall reduced Nusselt number, after replacing the solution given by Eq. (33) and using the relationships (35–39), is then given by

$$\overline{Nu} = \frac{\alpha}{\varepsilon^2}\left[1 - \frac{2k(1+\beta)}{3\beta}\frac{\alpha}{\varepsilon^2} + \frac{3kH(\beta)}{2\beta}\frac{\alpha^2}{\varepsilon^4} + \cdots\right] \tag{40}$$

where

$$H(\beta) = \frac{4}{3}\frac{1}{B(\frac{2}{3}, \frac{2}{3})} + \frac{1}{B(\frac{4}{3}, \frac{2}{3})}\left(\beta + \frac{1}{\beta}\right) - 4\sum_{n=1}^{\infty}\frac{c_n}{2n+3}$$

B. Asymptotic Limit $\beta \to \infty$

In this limit, the thermal resistance of the fluid II facing at the lower surface of the plate is very small and the nondimensional temperature at this surface diverges from zero in a quantity of order β^{-1}. The leading term corresponds to the solution of the convective problem with the lower surface of the plate with a uniform temperature $T_d = T_{II\infty}$ or in nondimensional form $\theta_d = 0$. This problem, for the thermally thick wall regime, is already classical and has been studied in several works.[1–5,13,14] For this limit it is appropriate to redefine the nondimensional temperature at the lower surface of the plate as $\varphi_d(\chi) = \theta_d(\chi)/\beta$. The governing Eqs. (32) reduce in this limit to

$$\begin{aligned} \theta_u - \frac{1}{\beta}\varphi_d &= -\frac{\varepsilon^2}{\alpha}\frac{1}{\sqrt{\chi}}\left(\int_0^{\chi} K_u\frac{d\theta_u'}{d\chi'}\,d\chi'\right) \\ &= \frac{\varepsilon^2}{\alpha\sqrt{1-\chi}}\left(\int_1^{\chi} K_d\frac{d\varphi_d'}{d\chi'}\,d\chi'\right) \end{aligned} \tag{41}$$

with the conditions $\theta_u(0) = 1$ and $\varphi_d(1) = 0$. The solution to Eqs. (41) can be obtained using the following expansions:

$$\theta_u = \sum_{j=0}^{\infty}\frac{\theta_{uj}}{\beta^j} \quad \text{and} \quad \varphi_d = \sum_{j=1}^{\infty}\frac{\varphi_{dj}}{\beta^j} \tag{42}$$

Introducing Eqs. (42) into Eqs. (41) we obtain after collecting terms with the same power of β

$$\theta_{u0} = -\frac{\varepsilon^2}{\alpha}\frac{1}{\sqrt{\chi}}\left(\int_0^{\chi} K_u\frac{d\theta_{u0}'}{d\chi'}\,d\chi'\right)$$

with the condition $\theta_{u0}(0) = 1$ (43)

$$\theta_{u0} = \frac{\varepsilon^2}{\alpha\sqrt{1-\chi}}\left(\int_1^{\chi} K_d\frac{d\varphi_{d1}'}{d\chi'}\,d\chi'\right)$$

with the condition $\varphi_{d1}(1) = 0$ (44)

$$\theta_{u1} - \varphi_{d1} = -\frac{\varepsilon^2}{\alpha}\frac{1}{\sqrt{\chi}}\left(\int_0^{\chi} K_u\frac{d\theta_{u1}'}{d\chi'}\,d\chi'\right)$$

with the condition $\theta_{u1}(0) = 0$ (45)

The leading term integral Eq. (43) is a parameter-free universal parabolic equation with $\xi = \chi\alpha^2/\varepsilon^4$ and serves to obtain the leading term of the nondimensional temperature at the upper surface of the plate, for a uniform isothermal lower surface of the plate. The solution to this equation can be found elsewhere.[2] For small values of ξ, the solution is given by the following series expansion:

$$\theta_{u0} = 1 - k\sqrt{\xi} + \frac{3k}{4B(\frac{4}{3}, \frac{2}{3})}\xi + \mathcal{O}(\xi^{3/2}) \quad \text{for} \quad \xi \to 0$$

Once θ_{u0} is obtained, the first-order correction of the nondimensional temperature at the lower surface of the plate φ_{d1} can be obtained from the solution of the integral Eq. (44). The first-order correction for the nondimensional temperature at the upper surface is obtained from the solution of the integral Eq. (45), etc.

V. Results and Comparison with Numerical Solution

The numerical results are obtained with the aid of the numerical code described elsewhere.[12] The Laplace Eq. (11) is numerically integrated using central differences in both directions. All of the first derivatives for the boundary conditions are evaluated using three points. The integral term of the boundary conditions (13) and (14) is discretized in the following form:

$$\begin{aligned} \int_0^{\chi} K_u\frac{d\theta'}{d\chi'}\,d\chi' &\simeq \sum_{k=1}^{i-1}\frac{(\theta_{k+1,M} - \theta_{k,M})}{\Delta\chi}\int_{(k-1)\Delta\chi}^{k\Delta\chi}\frac{d\chi'}{[1-(\chi'/\chi)^{3/4}]^{1/3}} \\ &= \frac{4\chi}{3\Delta\chi}\sum_{k=1}^{i-1}(\theta_{k+1,M} - \theta_{k,M})\int_{[(k-1)/(i-1)]^{3/4}}^{[k/(i-1)]^{3/4}}\frac{u^{\frac{1}{3}}\,du}{(1-u)^{1/3}} \\ &= \frac{4(i-1)}{3}\sum_{k=1}^{i-1}(\theta_{k+1,M} - \theta_{k,M})\left\{\beta\left[\frac{4}{3}, \frac{2}{3}\left(\frac{k}{i-1}\right)^{3/4}\right]\right. \\ &\quad \left. - \beta\left[\frac{4}{3}, \frac{2}{3}\left(\frac{k-1}{i-1}\right)^{3/4}\right]\right\} \end{aligned} \tag{46}$$

where $\beta(m, n, r)$ corresponds to the incomplete Beta function. Using this code, Fig. 2 shows the nondimensional transversal temperature difference at the wall $\theta_u(\chi = 0) - \theta_d(\chi = 0)$ for different values of the parameter α/ε^2. Here, we can see that for large values of $\alpha/\varepsilon^2 >> 1$, the nondimensional temperature difference is very small, which justifies the use of the thermally thin wall approximation. The main results and the comparison between the asymptotic and numerical analysis is displayed through Figs. 3–8. Taken into account that in heat transfer analysis the most relevant quantities are generally global, Figs. 3 and 4 give the corresponding average or overall reduced-Nusselt number as a function of α/ε^2 and different values of

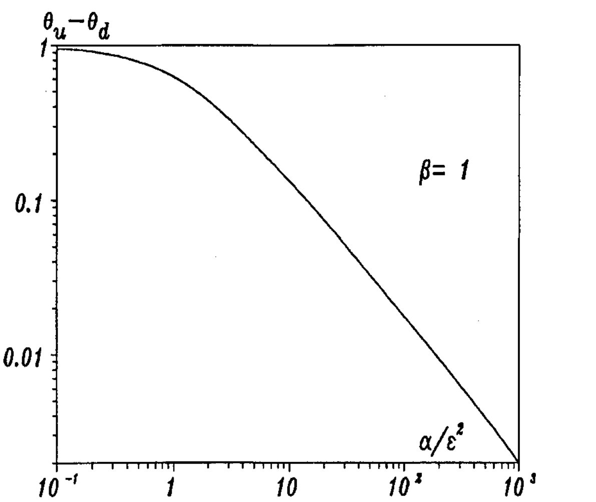

Fig. 2 Nondimensional transversal temperature of the plate at $\chi = 0$, for $\beta = 1$ and $\varepsilon = 0.1$.

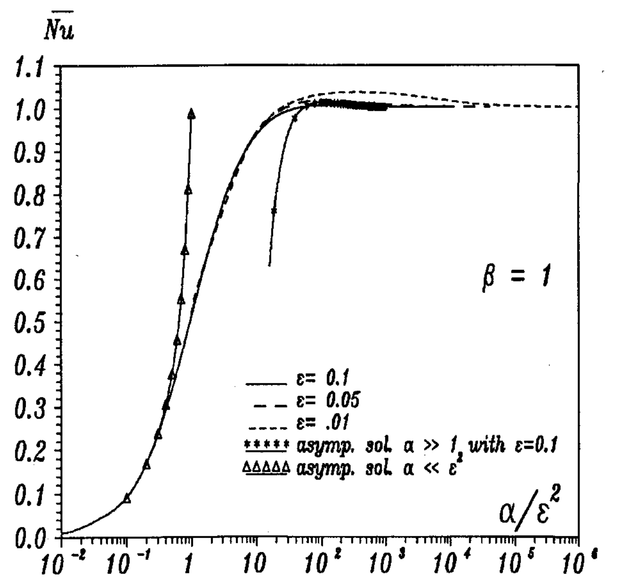

Fig. 3 Numerical and asymptotic average reduced Nusselt numbers as a function of α/ε^2 for $\beta = 1$.

β and ε. In both figures from the numerical predictions, we can see that for small and large values of α/ε^2, the average Nusselt number is independent of the values of ε and the influence is only detectable in a relatively small region of α/ε^2 of order unity, where the average Nusselt number shows a small but noticeable hump for $\beta = 1$. This hump disappears for values of $\beta >> 1$. The most direct result is that the maximum value of average Nusselt number occurs practically for values of α/ε^2 close to 100. Therefore, this unique feature of the solution, where the influence of the parameter ε is amplified by the overall Nusselt number, introduces a novel behavior in heat exchanger studies. Otherwise, for very large or very small values of α/ε^2, the average asymptotic and numerical Nusselt numbers have a universal form with respect to the parameter ε. The asymptotic expansions developed for small and large values of α/ε^2, show a relatively good agreement with the numerical results for values of β of order unity. However, as shown in Fig. 4, for large values of β, the thermally thin wall approximation isn't justified and a different approach is needed. Only the leading term of this approximation is valid. The asymptotic solution for the thermally thin wall limit could be plotted in Figs. 3 and 4, by using an artificial value of $\varepsilon = 0.1$, because this solution is not a function of ε, but is needed to plot both limits in one graph.

Finally, the comparison between the numerical and asymptotic analysis is given in Figs. 5–8, for the nondimensional temperature in the symmetrical middle plane of the plate (Figs. 5 and 6), for the lower surface ($z = -1$) in Fig. 7 and for the upper surface ($z = 0$) in Fig. 8, for different values of α, and β with $\varepsilon = 0.1$. The solution for values of $\beta < 1$, can be inferred from that of $\beta > 1$ using the following invariance transformation:

$$\begin{array}{lll} \beta \Rightarrow (1/\beta), & \alpha \Rightarrow (\alpha/\beta), & \theta_w \Rightarrow 1 - \theta_w \\ z \Rightarrow 1 - z, & \chi \Rightarrow 1 - \chi, & I \Leftrightarrow II \end{array} \tag{47}$$

In Figs. 5 and 6, the asymptotic limit of α large is considered but the corresponding value of β is different. As we can see in both figures, the agreement between the numerical estimation of the temperature and the three terms expansion is sufficient to describe the general behavior, and again, the influence of the parameter β is to make the temperature lower for higher values of β. On the other hand, it is clear that the non-

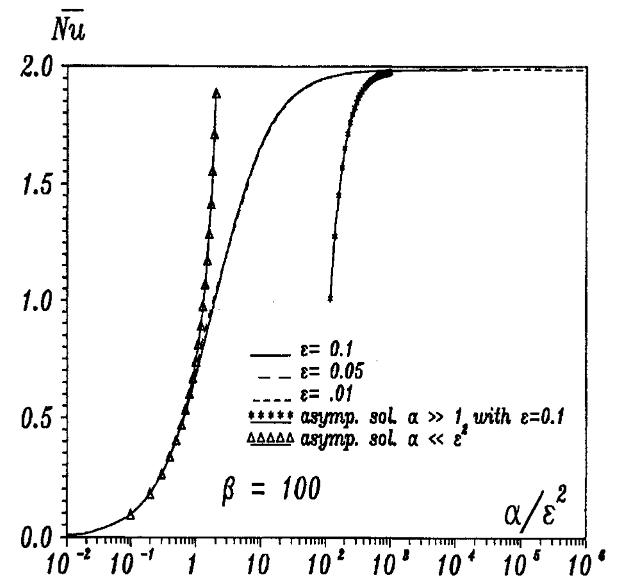

Fig. 4 Numerical and asymptotic average reduced Nusselt numbers as a function of α/ε^2 for $\beta = 100$.

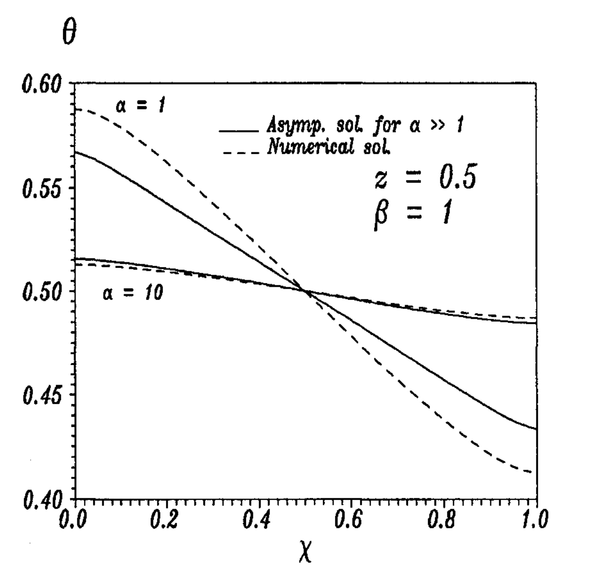

Fig. 5 Numerical and asymptotic solution for the nondimensional temperature distribution at $z = 0.5$ as a function of the nondimensional coordinate χ for $\beta = 1$, $\varepsilon = 0.1$, and $\alpha = 1$ and 10.

dimensional temperature shows a decreasing behavior for increasing values of the coordinate χ for fixed values of the parameters α, β, and ε. In the limit $\alpha << \varepsilon^2$, Fig. 7 shows the corresponding comparison at the lower surface. As we can see from this figure, the temperature at the lower surface of the plate is practically the same as the freestream temperature of the lower fluid *II*, as the value of β increases. An excellent agreement between numerical and asymptotic solutions is obtained. Figure 8 shows the numerical solution at the upper surface of the plate for $\alpha = 0.0001$ and two different values of β, and the asymptotic solution for $\beta = 1$. As we can see, the temperature at the upper surface is almost insensitive of the parameter β, for very small values of α/ε^2. This behavior is expected from Eqs. (33) and (34) because the influence of β in θ_u appears in the order of α^2/ε^4, whereas in θ_d it appears in the order of α/ε^2. We again obtain a very good agreement between the numerical and asymptotic results for this value of α. There is a small discrepancy in regions close to $\chi \to 0$, because of the existence of a thin layer where longitudinal heat conduction must be retained to satisfy the adiabatic boundary condition.

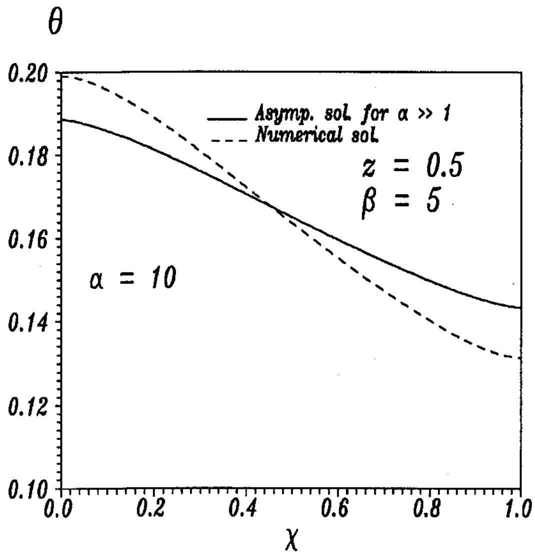

Fig. 6 Numerical and asymptotic solution for the nondimensional temperature distribution at $z = 0.5$ as a function of the nondimensional coordinate χ for $\beta = 5$, $\varepsilon = 0.1$, and $\alpha = 10$.

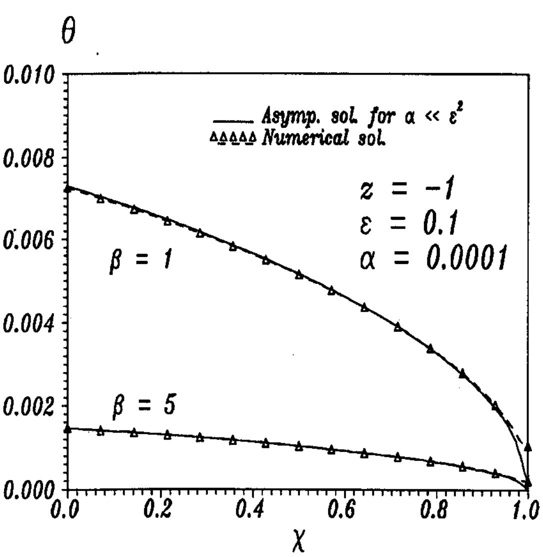

Fig. 7 Numerical and asymptotic solution for the nondimensional temperature distribution at the lower surface as a function of the nondimensional coordinate χ for $\beta = 1$ and 5, $\varepsilon = 0.1$, and $\alpha = 0.0001$.

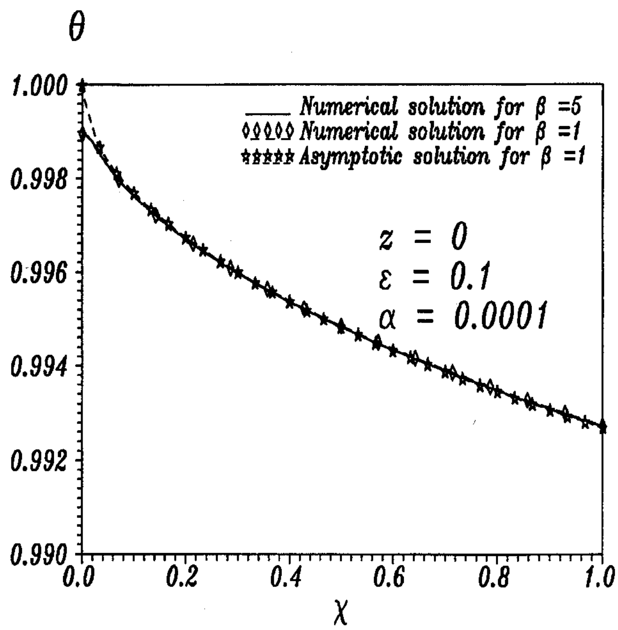

Fig. 8 Numerical solution for the nondimensional temperature distribution at the upper surface as a function of the nondimensional coordinate χ for $\beta = 1$ and 5, $\varepsilon = 0.1$, and $\alpha = 0.0001$. The asymptotic solution for $\beta = 1$ is also plotted.

VI. Conclusions

In this work we present the numerical solution and asymptotic analyses to study the heat transfer process between two counterflowing forced flows at different temperatures, separated by a flat plate. In both fluids we have used the Lighthill approximation for high Prandtl numbers, although it is a reasonable approximation for Prandtl numbers of order unity. The influence of the parameters α, β, and ε on this process has been analyzed. Because of the presence of these two boundary layers, the mathematical structure of the problem is elliptic, even for α equal to zero. The numerical and asymptotic results reflect very interesting facts in these kinds of multilayered heat exchangers: from the numerical point of view, the average Nusselt number is very sensitive to the changes for these parameters (α, β, and ε), and the solution can modify from one universal to a particular behavior, depending strongly on the values of the parameter α/ε^2. The importance of using asymptotic analysis is to obtain explicitly the distributions of the nondimensional temperature, local Nusselt number, and the average Nusselt number. From the analytical point of view, we have developed two important limits. The limits of large and small values of α are related to the limits of good and poor conducting plates, respectively.

Acknowledgment

This work has been supported by a grant of DGAPA, Univerídad Nacional Autonoma De Mexico IN107795.

References

[1]Luikov, A. V., "Conjugate Convective Heat Transfer Problems," *International Journal of Heat and Mass Transfer*, Vol. 17, 1974, pp. 257–265.

[2]Payvar, P., "Convective Heat Transfer to Laminar Flow over a Plate of Finite Thickness," *International Journal of Heat and Mass Transfer*, Vol. 20, 1977, pp. 431–433.

[3]Lighthill, M. J., "Contributions to the Theory of Heat Transfer Through a Laminar Boundary Layer," *Proceedings of the Royal Society of London*, Vol. A202, 1950, p. 359.

[4]Sohal, M. S., and Howell, J. R., "Determination of Plate Temper-

ature in Case of Combined Conduction, Convection and Radiation Heat Exchange," *International Journal of Heat and Mass Transfer*, Vol. 16, 1973, pp. 2055–2066 .

[5]Karvinen, R., "Some New Results for Conjugated Heat Transfer in a Flat Plate," *International Journal of Heat and Mass Transfer*, Vol. 21, 1978, pp. 1261–1264.

[6]Treviño, C., and Liñán, A., "External Heating of a Flat Plate in a Convective Flow," *International Journal of Heat and Mass Transfer*, Vol. 27, No. 7, 1984, pp. 1067–1073.

[7]Vallejo, A., and Treviño, C., "Convective Cooling of a Thin Flat Plate in Laminar and Turbulent Flows," *International Journal of Heat and Mass Transfer*, Vol. 33, No. 3, 1990, pp. 543–554.

[8]Stein, R. P., "The Graetz Problem in Cocurrent-Flow, Double-Pipe, Heat Exchangers," ANL Rept. 6889, 1964.

[9]Nunge, R. J., and Gill, W. N., "An Analytical Study of Laminar Counterflow Double-Pipe Heat Exchanger," *AIChE Journal*, Vol. 12, 1966, p. 279.

[10]Nunge, R. J., Porta, E. W., and Gill, W. N., "Axial Conduction in the Fluid Streams of Multistream Heat Exchangers," *Chemical Engineering Progress Symposium Series*, Vol. 63, No. 77, 1967, p. 80.

[11]Mori, S., Kataya, M., and Tanimoto, A., "Performance of Counterflow, Parallel Plate Heat Exchangers Under Laminar Flow Conditions," *Heat Transfer Engineering*, Vol. 2, No. 1, 1980, pp. 28–38.

[12]Medina, M., Luna, E., and Treviño, C., "Numerical Solution of the Conjugate Heat Transfer Between Forced Counterflowing Streams," *Heat and Mass Transfer*, Vol. 30, 1995, pp. 297–302.

[13]Pozzi, A., and Lupo, M., "The Coupling of Conduction with Forced Convection over a Flat Plate," *International Journal of Heat and Mass Transfer*, Vol. 23, 1989, pp. 1207–1214.

[14]Pop, I., and Ingham, D. B., "A Note on Conjugate Forced Convection Boundary-Layer Flow Past a Flat Plate," *International Journal of Heat and Mass Transfer*, Vol. 36, No. 15, 1993, pp. 3873–3876.